Competition between predissociative and radiative decays in the $e\,^3\Sigma_u^+$ and $d\,^3\Pi_u^-$ states of H_2 and D_2

Tatsuro Kiyoshima and Sugiya Sato
Laboratory of Physics, Nippon Institute of Technology, Miyashiro-Machi, Saitama 345, Japan

Sergey O. Adamson, Elena A. Pazyuk, and Andrey V. Stolyarov
Department of Chemistry, Moscow State University, Moscow, 119899, Russia
(Received 3 May 1999)

Experimental and theoretical lifetimes $\tau_{v'N'}$ for $e\,^3\Sigma_u^+$ and $d\,^3\Pi_u^-$ states of molecular hydrogen and deuterium are presented in a wide range of vibrational v' and rotational N' quantum numbers. Lifetimes have been measured by a delayed coincidence method following electron-impact excitation from the ground state. The cascade effects on the lifetimes measured were estimated to be negligible through a detailed analysis. Predissociative rates were estimated by the Fermi golden rule based on adiabatic rovibronic wave functions and radial coupling matrix elements $B(R)$ for the $e\,^3\Sigma_u^+ \sim b\,^3\Sigma_u^+$ and $d\,^3\Pi_u^- \sim c\,^3\Pi_u^-$ pairs of interacting states. The radiative lifetimes of both excited states were evaluated by the theoretical $e\,^3\Sigma_u^+ - a\,^3\Sigma_g^+$ and $d\,^3\Pi_u - a\,^3\Sigma_g^+$ transition dipole moment functions $d(R)$ and adiabatic rovibronic wave functions of the states involved. The electronic matrix elements $B(R)$ and $d(R)$ were obtained by direct *ab initio* calculations as well as within the framework of quantum defect theory. The *ab initio* $B(R)$ functions were calculated by the finite-difference method and by the analytical Sidis formula, which were based on the full configuration-interaction electronic wave functions. At small and medium internuclear distances the quantum defect matrix elements agree well with their *ab initio* counterparts. The predissociative rates for both $e\,^3\Sigma_u^+(v' \geqslant 0)$ and $d\,^3\Pi_u^-(v' \geqslant 4)$ states of hydrogen were found to increase sharply as the v' value of the predissociated level increases, and become compatible with the radiative decay rate. The predissociation effect in the deuterium was negligible for both states studied; hence their experimental lifetimes correspond to the radiative decay channel only. A sum of the theoretical radiative and predissociative rates was in good agreement with the experimental results for the $e\,^3\Sigma_u^+$ state but slightly overestimated for the $d\,^3\Pi_u^-$ state. Reasons for the remaining discrepancies are discussed and suggestions for further improvements are given.
[S1050-2947(99)10212-9]

PACS number(s): 33.70.−w

I. INTRODUCTION

Highly accurate energy and dynamic properties of the excited states of molecular hydrogen are needed to diagnose low-temperature molecular plasmas [1] and the atmospheres of the Jovian planets [2]. In particular, the rovibronic transition probabilities are certainly required in order to perform a population analysis of the molecular excited states and to determine the gas temperature [3]. However, strong coupling of the electronic and nuclear motions in electronically excited hydrogen states manifests numerous competitions between different intramolecular processes which proceed beyond the Born-Oppenheimer (BO) approximation [4,5]. From experimental and theoretical viewpoints, behaviors of the ungerade triplet $3p$ complex $e\,^3\Sigma_u^+$ and $d\,^3\Pi_u$ states of molecular hydrogen are very attractive patterns because their transition channels such as radiative transition to the $a\,^3\Sigma_g^+$ state, predissociation through the $b\,^3\Sigma_u^+$ and $c\,^3\Pi_u^-$ states as well as the mutual perturbation of the $e\,^3\Sigma_u^+$ and $d\,^3\Pi_u^+$ states are in a strong competition.

Regular and local L uncoupling effects on the term values of the $d\,^3\Pi_u^+$ and $e\,^3\Sigma_u^+$ states [6–8], and the relative intensity distributions in emission of the $d\,^3\Pi_u \rightarrow a\,^3\Sigma_g^+$ and $e\,^3\Sigma_u^+ \rightarrow a\,^3\Sigma_g^+$ bands [3,9–13], have been extensively investigated in both H_2 and D_2 molecules. Numerous direct lifetime measurements in the $d\,^3\Pi_u(v' \leqslant 3)$ rovibronic levels have also been reported [14–16]. The empirical $d\,^3\Pi_u - a\,^3\Sigma_g^+$ and $e\,^3\Sigma_u^+ - a\,^3\Sigma_g^+$ transition dipole moment functions were derived by deperturbation analysis of the available experimental data [11–13], and the radiative lifetime of the $e\,^3\Sigma_u^+$ state was predicted to be 39–47 ns [3,10]. Kiyoshima and Sato [16][1] investigated the strong local $d\,^3\Pi_u^+ \sim e\,^3\Sigma_u^+$ perturbation effect on the lifetimes of $d\,^3\Pi_u^+(v' = 1)$ rovibronic levels. Based on a systematic lifetime variation of the $d\,^3\Pi_u^+$ levels with the rotational quantum number N', they estimated that the predissociative lifetime for the $e\,^3\Sigma_u^+(v' = 4)$ level of H_2 should be 3.7 (0.8) ns [16] whereas the $e\,^3\Sigma_u^+$ state of D_2 is not predissociated at all. Furthermore, Burshtein *et al.* [15] showed that the lifetimes of $d\,^3\Pi_u^-(v' = 4,5,6)$ levels are much shorter than those for $v' \leqslant 3$ levels and ascribed it, without any theoretical treatment, to predissociation effect. For the $e\,^3\Sigma_u^+$ levels, however, neither direct lifetime measurements nor theoretical calculations of the radiative and predissociative rates have been carried out, though experiments of light emissions [6]

[1] $^1\Pi^e$ and $^1\Pi^f$ used as the Λ-doublet symbols in Ref. [16] should be replaced by $^1\Pi^-$ and $^1\Pi^+$, respectively.

and time of flight of dissociation fragments [17] have been reported.

Highly accurate BO potential curves together with the corresponding adiabatic corrections calculated by highly flexible variational wavefunctions are known for all $^3\Sigma^+$ states considered in the present work [18,19]. A highly accurate BO potential for the $c\,^3\Pi_u$ state is also available [20]. However, regarding the $d\,^3\Pi_u$ state, there is only the BO potential derived by the conventional *ab initio* calculation with a small Gaussian-type orbital (GTO) basis set [21]. The adiabatic corrections for both $^3\Pi_u$ states remain uncalculated. The radial coupling matrix elements $B(R)$ between the lowest $^3\Sigma_u^+$ states were estimated in Ref. [22] from the model *ab initio* calculations. No theoretical attempt has been made to calculate the *d-a* and *e-a* transition dipole moment functions.

The main goal of this study is to elucidate the radiation and predissociation processes for $d\,^3\Pi_u^-$ and $e\,^3\Sigma_u^+$ states. We present a comparison between experimental and theoretical lifetimes for the $d\,^3\Pi_u^-$ and $e\,^3\Sigma_u^+$ states of H_2 and D_2 molecules. The theoretical results were obtained based on the assumed competition between the radiative ($e\,^3\Sigma_u^+ \rightarrow a\,^3\Sigma_g^+$; $d\,^3\Pi_u \rightarrow a\,^3\Sigma_g^+$) transitions and predissociations caused by the radial ($e\,^3\Sigma_u^+ \sim b\,^3\Sigma_u^+$; $d\,^3\Pi_u^- \sim c\,^3\Pi_u^-$) coupling. Although the L uncoupling of the $e\,^3\Sigma^+$ and $d\,^3\Pi^+$ states as well as fine and hyperfine interactions were ignored throughout the study, we believe that this work is a step forward understanding dynamical properties of the ungerade triplet $3p$ complex states of molecular hydrogen.

II. EXPERIMENT AND DATA ANALYSIS

Lifetimes were measured by a delayed coincidence method. The experimental setup was similar to that described in Ref. [16]. Briefly, the rovibronic levels of $d\,^3\Pi_u$ and $e\,^3\Sigma_u^+$ states in H_2 and D_2 were populated by electron-impact excitation. The electron beams, generated by an electron gun equipped with an oxide cathode, had 30–50-eV energy and 10–30-μA current. They were modulated by adding rectangular voltage pulses of 200-ns width, 5-ns fall time, and 100-kHz repetition frequency to the grid electrode which was biased deeply enough to cut off the electron beam. The ultimate vacuum 10^{-5} Pa of the vacuum chamber was produced by an oil diffusion pump. The target gases were introduced through a capillary nozzle into an electron-molecule collision cage, and differentially pumped out. Thus the pressure in the cage was maintained at 1.2 Pa. We ascertained that the errors arising from the collision effects on the lifetimes measured were negligible at this pressure. We measured the lifetimes of $d\,^3\Pi_u$ and $e\,^3\Sigma_u^+$ levels by detecting the photons from $d\,^3\Pi_u - a\,^3\Sigma_g^+$ (wavelength range 6300–6650 Å) and $e\,^3\Sigma_u^+ - a\,^3\Sigma_g^+$ (5900–8550 Å) bands, respectively. The photons emitted in a direction perpendicular to the electron beam were focused by a concave mirror and a quartz lens onto the entrance slit of a monochromator with a 1-m focal length. After being dispersed by the monochromator, the selected photons were detected by a cooled photomultiplier. Two types of photomultipliers (HAMAMATSU, R649, and R2257P) were used for the photon detection in the above wavelength range. We obtained line widths of 0.8-Å full width at half maximum (FWHM) in the region studied. We identified each line belonging to $d\,^3\Pi_u^- - a\,^3\Sigma_g^+$ and $e\,^3\Sigma_u^+ - a\,^3\Sigma_g^+$ bands by the wavelength tables of Dieke [7] for H_2 and Freund *et al.* [8] for D_2. The lines selected for lifetime measurement are shown in Table I. Blending components to these lines were negligible. The time intervals between molecular excitation and photon detection were converted to voltage pulses by a time-to-amplitude converter and distributed in a 512-channel pulse-height analyzer connected to a computer. The interval between neighboring channels was 1.89 ns. A typical decay curve is shown in Fig. 1.

TABLE I. The experimental and theoretical ($\tau^{-1} = \tau_{\rm rad}^{-1} + \tau_{\rm pred}^{-1}$) lifetimes (in ns) of H_2 $e\,^3\Sigma_u^+$ and $d\,^3\Pi_u^-$ levels. The theoretical $\tau_{\rm rad}$ was derived based on the *ab initio* dipole moments, and $\tau_{\rm pred}$ based on the coupling matrix elements calculated by the *ab initio* FDT method.

v'	N'	v''	Branch	Experimenal (error)	Calculated (error)
				$e\,^3\Sigma_u^+$ state	
0	2	0	R	33.9 (3.8)	30.7 (0.5)
1	2	0	R	30.3 (1.1)	24.6 (1.0)
2	0	0	P	16.1 (1.6)	13.7 (0.5)
2	2	0	R	11.9 (1.4)	14.4 (0.5)
3	0	1	P	7.6 (0.5)	7.4 (0.5)
3	2	1	R	10.4 (0.7)	7.8 (0.5)
4	1	2	R	4.7 (1.2)	4.7 (0.5)
4	2	2	P	5.4 (0.7)	4.9 (0.4)
4	3	2	R	11.5 (0.6)	5.1 (0.4)
5	2	2	R	4.5 (1.5)	3.3 (0.4)
				$d\,^3\Pi_u^-$ state	
4	1	4	Q	16.0(0.6)	9.9(0.5)
4	3	4	Q	16.6(0.7)	10.5(0.5)
5	1	5	Q	11.5(0.6)	7.3(0.3)
5	2	5	Q	12.3(0.9)	7.5(0.3)
5	3	5	Q	10.9(0.9)	7.8(0.3)
6	1	6	Q	10.2(0.4)	5.6(0.3)
6	3	6	Q	11.3(5.3)	5.9(0.3)

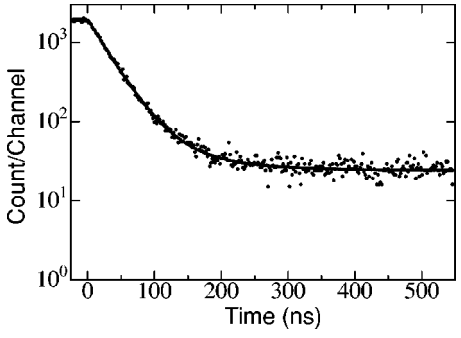

FIG. 1. The decay curve recorded for the $e\,^3\Sigma_u^+(v'=1) \rightarrow a\,^3\Sigma_g^+(v''=0)$ $R(1)$ line in H_2. The decay function is assumed to be $A_1 e^{-t/\tau_1} + A_2 e^{-t/\tau_2} + B$. The solid line shows a convolution of the decay function and an apparatus function. The fitting parameters: $\tau_1 = 30.3 \pm 1.1$ (ns) is a lifetime of the $e\,^3\Sigma_u^+(v'=1; N'=2)$ level, $\tau_2 = 82 \pm 23$ (ns) is a long-lived component, and $A_2/A_1 = 0.08 \pm 0.02$.

A lifetime was determined from each decay curve by the following procedures. First, we performed a multiexponential fitting with the program DISCRETE [23] which gave the most probable number of components and their fitting parameters. Then we selected data which had one component or a true component plus a long-lived one. Next we defined a convolution of one or two exponents with Gaussian apparatus function [24] of an appropriate width in the range 3.6–6.4-ns FWHM, and then, this was fitted to the decay curve using the results of DISCRETE as the initial values for the least-square fitting. The last procedure allowed one to include data around the excitation cutoff time ($t=0$) into analysis. The fitting was made in the range of $0 \leqslant t \leqslant 756$ ns. The errors of derived lifetimes consist of statistical errors in the individual fits, scatter among the independent measurements, and errors arising from uncertainties of the time origin. We estimated the influence of cascade transitions on the present lifetimes to be negligible by the following reasons. (1) The most reliable candidate to give cascade effects on the $e\,^3\Sigma_u^+$ or $d\,^3\Pi_u$ lifetimes measured is gerade triplet $3s,d$ complex ($g\,^3\Sigma_g^+$, $h\,^3\Sigma_g^+$, $i\,^3\Pi_g$, $j\,^3\Delta_g$) because their radiative lifetimes (6–16 ns) [25,26] are comparable with those measured. However, recent investigations show that the decay branching ratios from the complex to $e\,^3\Sigma_u^+$ levels are much smaller than those to $c\,^3\Pi_u$ or $b\,^3\Sigma_u^+$ [25,26]. The decay branching ratios from the complex to the $d\,^3\Pi_u^-$ levels are considered to be negligible due to the very small energy gap between the complex and $d\,^3\Pi_u^-$ state. (2) We carefully analyzed the decay curves recorded for the H_2 $e\,^3\Sigma_u^+(1,0)R(1)$ line by the program DISCRETE varying the starting time of analysis over a wide range. As a result, no negative amplitude component was found. Hence, any cascade component whose lifetime is shorter than the true one does not exist in the spectrum [27]. (3) After analyses by the program DISCRETE, we selected data consisting of positive-amplitude components alone. The long-lived components observed in the two-component spectra could be easily separated.

III. OUTLINE OF THEORY

A. Radiative and predissociative lifetimes

The schema of potential curves presented in Fig. 2 and well-known selection rules for radiative and nonradiative diatomic transitions [5] show two possible decay channels for the rovibronically excited $e\,^3\Sigma_u^+$ and $d\,^3\Pi_u^-$ states of molecular hydrogen. The first is the famous radiative decay into the rovibrational terms of the lower $a\,^3\Sigma_g^+$ state by emitting a photon quanta: $e\,^3\Sigma_u^+; d\,^3\Pi_u^- \rightarrow a\,^3\Sigma_g^+ + h\nu$. The second is predissociative decay through the rovibrational continuum of the lower-lying $b\,^3\Sigma_u^+$ and $c\,^3\Pi_u^-$ states, respectively: $e\,^3\Sigma_u^+ \rightarrow b\,^3\Sigma_u^+ \rightarrow H(1s)+H(1s)$ and $d\,^3\Pi_u^- \rightarrow c\,^3\Pi_u^- \rightarrow H(1s)+H(2l)$.

Under collision and cascade free conditions a reciprocal value of the experimental lifetime is the sum of the radiative and predissociative channel rates: $\tau_{\rm expt}^{-1} = \tau_{\rm rad}^{-1} + \tau_{\rm pred}^{-1}$. The radiative lifetime $\tau_{\rm rad}(v',N')$ is [5]

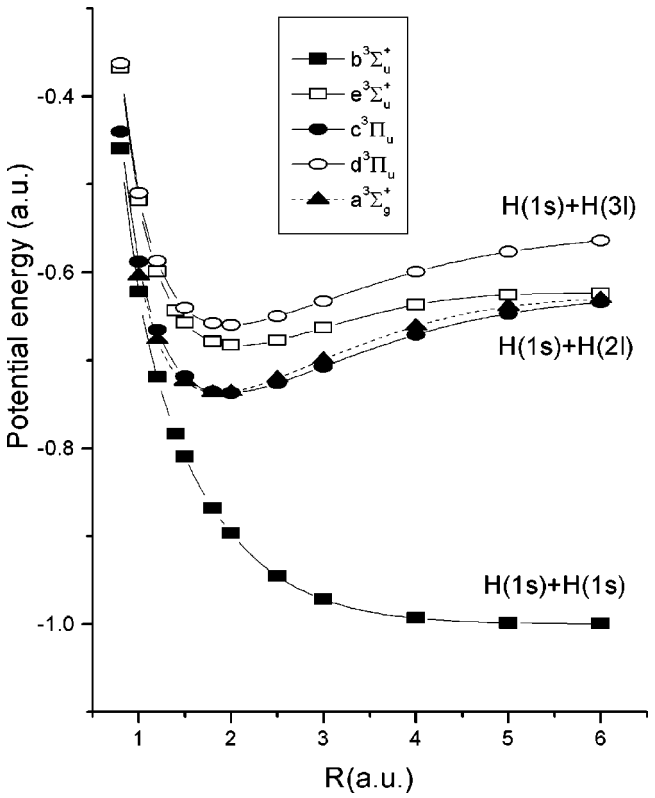

FIG. 2. The calculated Born-Oppenheimer potential-energy curves of the $b\,^3\Sigma_u^+$, $e\,^3\Sigma_u^+$, $c\,^3\Pi_u$, $d\,^3\Pi_u$, and $a\,^3\Sigma_g^+$ states of molecular hydrogen.

$$\tau_{\rm rad}^{-1} = \frac{64\pi^4}{3h} \sum_{v''N''} (\nu_{ij}^{v'N'v''N''})^3 |\langle \chi_{v'N'}(R)|d_{ij}(R)|\chi_{v''N''}(R)\rangle|^2 \times \frac{S_{N'N''}}{2N'+1}, \tag{1}$$

where $d_{ij}(R)$ is the transition dipole moment between the i and j electronic states, R is the internuclear distance, and ν_{ij} is the wave number of the $i-j$ transition. $S_{N'N''}$ is the Hönl-London factor, and the sum is over all the possible rotational and vibrational radiative decay channels. $\chi_{v'N'}(R)$ and $\chi_{v''N''}(R)$ are the vibrational wave functions (WF's) corresponding to the bound levels of the upper and lower states, respectively. The predissociative lifetime $\tau_{pred}(v',N')$ is approximated by [28]

$$\tau_{\rm pred}^{-1} = 4\pi^2 c \left| \frac{1}{2m} \langle \chi_{v'N'}(R)|2B_{ij}(R)\frac{d}{dR}|\chi_{E''N''}(R)\rangle \right|^2, \tag{2}$$

where m is the reduced molecular mass and $B_{ij}(R)$ is the nonadiabatic electronic matrix element of the radial coupling. Here $\chi_{v'N'}(R)$ and $\chi_{E''N''}(R)$ are the vibrational WF's corresponding to the bound and continuum levels of the interacting electronic states, respectively. Thus, in the present adiabatic approximation, the radial coupling and transition moment matrix elements as a function of internuclear distance R and the relevant adiabatic vibrational WF's are sufficient to estimate both predissociative and radiative lifetimes.

B. Radial coupling and transition dipole-matrix elements

The radial coupling $B_{ij}(R)$ and transition dipole $d_{ij}(R)$ matrix elements in a homonuclear diatomic molecule are $B_{ij}=\langle\Psi_i^{\rm BO}|d/dR|\Psi_j^{\rm BO}\rangle$ and $d_{ij}=\langle\Psi_i^{\rm BO}|\Sigma_n r_n|\Psi_j^{\rm BO}\rangle$, where $\Psi_i^{\rm BO}(\mathbf{r},R)$ and $\Psi_j^{\rm BO}(\mathbf{r},R)$ are the BO electronic WF's of the i and j interacting states, r is the radial coordinate of the electron, and the sum is over all electrons. In the present work B_{ij} and d_{ij} electronic matrix elements have been estimated by direct *ab initio* calculations as well as in the framework of quantum defect theory (QDT) approximation [29].

1. Ab initio calculations

The required BO eigenvalues and eigenfunctions for all states under consideration have been computed by the full-configuration-interaction (FCI) method with contracted GTO basis set. The employed orbital basis was composed of the sets of the averaged atomic natural orbital $(8s4p3d)/[6s4p3d]$ centered on the H atoms [30] and augmented by the Rydberg-like s (exponential parameter $\zeta=0.01$), p ($\zeta=0.03,0.01$), and d ($\zeta=1,0.03,0.01$) functions on the center of masses. The d-a and e-a transition dipole moments were estimated in the dipole-length approximation. The radial coupling matrix elements for d-c and e-b pairs of the interacting states were calculated by the finite-difference technique (FDT) [31]

$$B_{ij}^{\Lambda}(R)=\lim_{\delta R\to 0}\langle\Psi_i^{\rm BO}(\mathbf{r},R-\delta R/2)|\Psi_j^{\rm BO}(\mathbf{r},R+\delta R/2)\rangle/\delta R \tag{3}$$

and by the Sidis formula [32]

$$B_{ij}^{\Lambda}(R)=\left[\langle\Psi_i^{\rm BO}|-\frac{1}{2}\Delta|\Psi_j^{\rm BO}\rangle/\Delta U_{ij}+\Delta U_{ij}\langle\Psi_i^{\rm BO}|\sum_n r_n^2|\Psi_j^{\rm BO}\rangle/2\right]\Big/ R, \tag{4}$$

where $-\frac{1}{2}\Delta$ is the electronic kinetic-energy operator and $\Delta U_{ij}=U_i^{\rm BO}(R)-U_j^{\rm BO}(R)$ is the difference between BO potential curves of the interacting states. The step of the numerical differentiation δR in FDT was selected to be 0.0001 a.u. for all internuclear distances, since the doubled increasing or decreasing of the present step size has been proven to give negligible variation in the resulting FDT $B_{ij}(R)$ values in the R region studied.

2. Quantum defect approximation

Analysis of the derived *ab initio* WF's shows their predominant Rydberg character at least at the small and medium internuclear distances. Indeed, the $b\,^3\Sigma_u^+$, $e\,^3\Sigma_u^+$, $c\,^3\Pi_u$, $d\,^3\Pi_u$, and $a\,^3\Sigma_g^+$ states have $2p\sigma$, $3p\sigma$, $2p\pi$, $3p\pi$ and $2s\sigma$ leading electronic configurations, respectively. This allows us to apply the QDT approximation to the present states. In the simplest one-channel representation the BO WF belonging to a given Rydberg electronic state with a fixed Λ value can be approximated as [29]

$$\Psi_{\Lambda}^{\rm BO}(\mathbf{r},R)=\Psi_{\Lambda^+}^{\rm BO}(\mathbf{r},R)Y_{l,\Lambda-\Lambda^+}(\vartheta,\varphi)P_{\Lambda}^{n,l}(r,R), \tag{5}$$

where $\Psi_{\Lambda^+}^{\rm BO}(\mathbf{r},R)$ is the BO ground electronic state WF of the positive core, $Y_{l,\Lambda-\Lambda^+}(\vartheta,\varphi)$ is the ordinary spherical harmonic function corresponding to the orbital factor of the remote electron, and l is the orbital angular momentum of the outer electron. Λ and Λ^+ are the projections of the electronic angular momentum operators $\mathbf{L}_z$ and $\mathbf{L}_{z,\rm ion}$ on the internuclear axis, respectively. The radial part of the Rydberg orbital $P_{\Lambda}^{n,l}(r,R)$ are available in the closed form [33]

$$P_{\Lambda}^{n,l}(r,R)=W_{\nu_n,l+1/2}(2r/\nu_n)/\nu_n\sqrt{\Gamma(\nu_n+l+1)\Gamma(\nu_n-l)}, \tag{6}$$

where $\nu_n(R)=n-\mu_{n,\Lambda}(R)$ is the *effective quantum number*, $\mu_{n,\Lambda}(R)$ is the *quantum defect function*, and Γ and W are the gamma and the Whittaker functions, respectively. The $\mu_{n,\Lambda}(R)$ functions may be obtained by a rearrangement of the Mulliken equation [34]

$$U_{nl\Lambda}^{\rm BO}(R)=U_{\Lambda^+}^{\rm BO}(R)-\frac{1}{2[n-\mu_{n,\Lambda}(R)]^2}, \tag{7}$$

where $U_{nl,\Lambda}^{\rm BO}$ and $U_{\Lambda^+}^{\rm BO}$ are the BO potential curves for molecular Rydberg states and the ground state of the ion, respectively. In the framework of the QDT approximation the $B_{ij}^{\Lambda}(R)$ and $d_{ij}^{\Lambda,\Lambda'}(R)$ matrix elements are given by the analytical forms [26,35]

$$B_{ij}^{\Lambda}(R)=\frac{2\mu_{\Lambda}'\sqrt{\nu_i\nu_j}}{\nu_i^2-\nu_j^2}, \tag{8}$$

$$d_{ij}^{\Lambda,\Lambda'}=\begin{pmatrix} l & 1 & l' \\ 0 & 0 & 0\end{pmatrix}\begin{pmatrix} l & 1 & l' \\ \Lambda^+-\Lambda & \Lambda-\Lambda' & \Lambda'-\Lambda^+\end{pmatrix}\times[(2l+1)(2l'+1)]^{1/2}S_{ij}, \tag{9}$$

where $\mu_{\Lambda}'=d\mu_{\Lambda}/dR$ and

$$S_{ij}(R)=(-1)^{\Lambda-\Lambda^+}\langle P_{\Lambda}^{n_i,l}|r|P_{\Lambda'=\Lambda,\Lambda\pm1}^{n_j,l'=l\pm1}\rangle$$

is the radial dipole matrix element. Hence only the $\mu_{n,\Lambda}(R)$ functions are needed to estimate $B_{ij}(R)$ and $d_{ij}(R)$ matrix elements. For each molecular state under consideration the $\mu_{n,\Lambda}(R)$ function was derived from Eq. (7) using the *ab initio* $U_{nl,\Lambda}^{\rm BO}$ obtained in the preceding subsection and the *ab initio* $U_{\Lambda^+}^{\rm BO}$ taken from Ref. [36]. The μ_{Λ}' values were calculated by an ordinary cubic spline interpolation of $\mu(R)$ values. The radial matrix elements $S_{ij}(R)$ were evaluated numerically by asymptotic expansion of the Whittaker function in Eq. (6) [37].

C. Potential curves, rovibrational wave functions, and matrix elements

The rovibrational energies E_{vN} and WF's $\chi_{vN}(R)$ for bound and continuum levels for all states studied were derived by a numerical solution of the radial Schrödinger equation

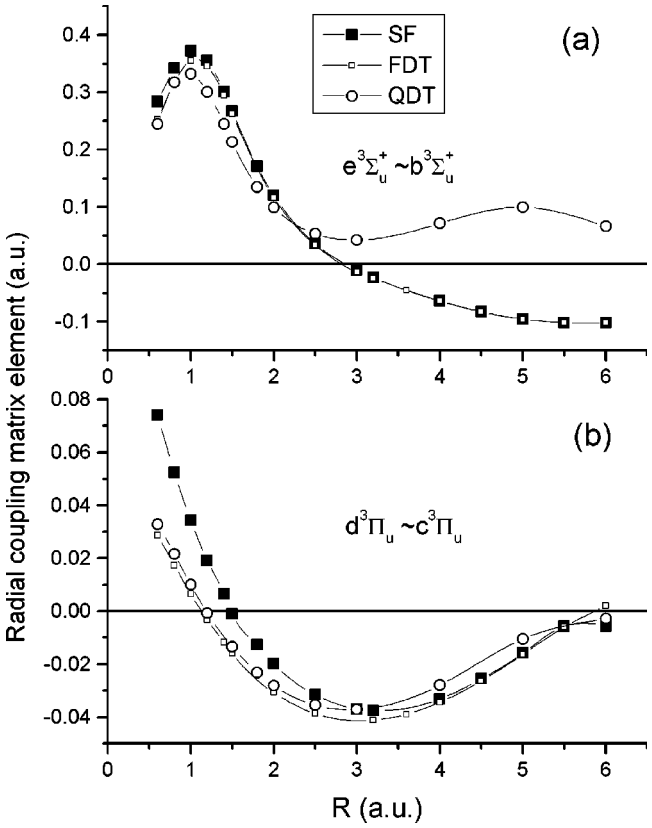

FIG. 3. The nonadiabatic $e\,^3\Sigma_u^+ \sim b\,^3\Sigma_u^+$ (a) and $d\,^3\Pi_u \sim c\,^3\Pi_u$ (b) radial coupling matrix elements calculated by the finite-difference technique (FDT) and the Sidis formula (SF) as well as those estimated in the framework of quantum defect theory (QDT).

$$\left[-\frac{1}{2m}\frac{d^2}{dR^2}+U_{\rm ad}(R)+\frac{N(N+1)}{2mR^2}-E_{vN}\right]\chi_{vN}(R)=0, \tag{10}$$

where $U_{\rm ad}(R)$ is the mass-dependent rotationless adiabatic potential based on the BO separation. Figure 2 shows that a predissociation of the rovibronic $e\,^3\Sigma_u^+$ and $d\,^3\Pi_u^-$ levels corresponds to c^0 case of the Mulliken's classification [38]. In this case the predissociation rate is expected to be exponentially small and extremely sensitive to the accuracy of the $\chi_{v'N'}(R)$ and $\chi_{E''N'}(R)$ vibrational WF's [5]. Hence, the most accurate adiabatic potentials (especially their repulsive walls) are needed to obtain a feasible magnitude of the rovibronic matrix elements of the predissociation. The required adiabatic potentials can be obtained from the direct highly accurate *ab initio* calculations of BO potential curves together with adiabatic corrections and also from the experimental rovibronic level positions either by a widespread Rydberg-Klein-Rees (RKR) method or by inverted perturbation approach (IPA) [39]. The semiclassical RKR inversion procedure is not ideally suited for the hydrogen isotopes due to their small reduced mass. The full quantum-mechanical IPA method is essentially more accurate than its RKR counterpart for all hydrogen states. In most practical cases the empirical IPA potentials are more accurate than their *ab initio* counterparts. However, an application of the RKR or IPA procedure is generally restricted to unperturbed electronic states. A comparison of the radial coupling matrix elements for the $^3\Sigma_u^+$ and $^3\Pi_u$ states presented in Fig. 3 shows that the $^3\Sigma_u^+$ states should be significantly more perturbed than the $^3\Pi_u$ states. Fortunately, highly accurate *ab initio* BO potentials together with the relevant adiabatic corrections are available for all Σ states under consideration [18,19]. For these reasons, the IPA potentials have been derived only for $d\,^3\Pi_u$ states of both H_2 and D_2 molecules. For the $c\,^3\Pi_u$ state the adiabatic potentials were evaluated by a combination of the highly accurate *ab initio* BO curve taken from Ref. [20] and adiabatic correction $A_{\rm ad}(R)$ estimated by the QDT approximation [35]:

$$A_{\rm ad}(R)=\frac{1}{2m}\left[A^{\rm ion}(R)-4(\mu')^2\sum_{j\neq i}^{\infty}\frac{\nu_i\nu_j}{(\nu_i^2-\nu_j^2)^2}-\frac{2R\mu'+\nu_i}{4\nu_i^3}\right], \tag{11}$$

where $A^{ion}(R)$ is the adiabatic correction for the ground state of the hydrogen ion [36]. The potential curves thus obtained for the states under study are shown in Fig. 2.

As is well known, the $B_{ij}d/dR$ operator is not Hermitian, so in practice the term dB_{ij}/dR should be added to make the total Hermitian operator. Indeed, since B_{ij} is anti-Hermitian, it can be easily proven by integration by parts that the equation

$$\left\langle \chi_i\left|2B_{ij}\frac{d}{dR}+\frac{dB_{ij}}{dR}\right|\chi_j\right\rangle=\left\langle \chi_j\left|2B_{ji}\frac{d}{dR}+\frac{dB_{ji}}{dR}\right|\chi_i\right\rangle \tag{12}$$

is valid. However, the left- and right-hand sides of Eq. (12) are not necessarily equal in actual calculations because of their limited accuracy. This means that both sides of the Eq. (12) can be used to control calculational accuracy.

To integrate Eq. (10) we implemented the iterative renormalized Numerov algorithm [40] combined with the Richardson extrapolation [41]. This construction allows one to reduce the absolute errors in rovibrational WF's to 10^{-5}. The continuum WF's were normalized in energy by the matching of a numerical eigenfunction to its quasiclassical counterpart at a large internuclear distance [28]. An efficient phase-matching method was employed to determine the eigenvalues of the bound states [42]. The ordinary cubic spline interpolation was used in Eq. (12) to estimate the first derivative of the vibrational WF's and B_{ij} matrix elements with respect to R.

IV. RESULTS AND DISCUSSION

The lifetimes measured and calculated for H_2 $e\,^3\Sigma_u^+(v'\geqslant 0)$ and $d\,^3\Pi_u^-(v'\geqslant 4)$ levels are shown in Table I. A comparison between the experimental and theoretical data over a wide range of the v' and N' values and for different isotopes are also shown in Figs. 5(a) and 5(b) and 7(a) and 7(b). It can be seen from Table I and Fig. 7(a) that the measured lifetimes of H_2 $e^3\Sigma_u^+$ levels generally decrease with v', while those of D_2 levels remain almost constant [see Fig 5(a)]. This strongly supports a conclusion of the previous work [16] in that some of the $e\,^3\Sigma_u^+$ levels are predissociated in H_2 but not in D_2. Moreover, it suggests that the lifetime variation

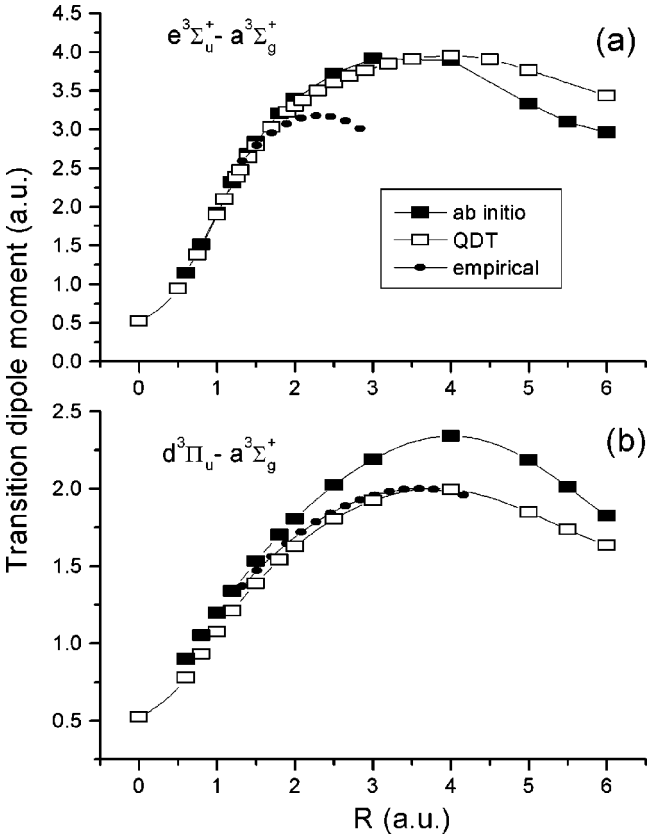

FIG. 4. The $e\,^3\Sigma_u^+ - a\,^3\Sigma_g^+$ (a) and $d\,^3\Pi_u - a\,^3\Sigma_g^+$ (b) transition dipole moment functions calculated directly from *ab initio* WF's in a dipole-length approximation and estimated by the quantum defect theory (QDT). Empirical moments were derived in Refs. [10,12] from the experimental relative intensity distributions in the *d-a* and *e-a* emission spectra.

with v' in the H_2 $e\,^3\Sigma_u^+$ state is attributed to predissociation by radial coupling between the $e\,^3\Sigma_u^+$ and repulsive $b\,^3\Sigma_u^+$ states because significantly shorter lifetimes are observed even for $N'=0$ levels at which the L-uncoupling predissociation should not occur [5]. It can also be seen in Table I and Fig. 7(b) that the lifetimes of the H_2 $d\,^3\Pi_u^-(v' \geqslant 4)$ states decrease abruptly in the energy range higher than the $H(1s)+H(2l)$ dissociation limit, which is in agreement with the results of Burshtein *et al.* [15], while those of D_2 $d^3\Pi_u^-(v' \geqslant 5)$ levels still remain almost constant, as seen in Fig. 5(b).

The resulting *ab initio* and QDT radial coupling matrix elements for the $^3\Sigma_u^+$ and $^3\Pi_u$ state pairs are presented in Figs. 3(a) and 3(b), respectively. The $B(R)$ functions obtained by FDT and Sidis formula almost coincide for Σ state pairs, but slightly disagree for Π state pairs at small internuclear distances. This means that the present *ab initio* WF's and energies are more accurate for Σ states than for Π states because the analytical Sidis approach is expected to be more sensitive to the accuracy of the BO energies and WF's than the FDT method [31]. This conclusion is confirmed by a direct comparison of the present BO curves with more accurate *ab initio* [18–20] and empirical IPA potentials; that is, the observed energy difference for all Σ states does not exceed 20–50 cm^{-1}, while for the Π states (and especially for the $d^3\Pi_u$ state) it reaches 150–200 cm^{-1}. Figures 3(a) and 3(b) show that the simple one-channel QDT approximation works better for Π states than for Σ states. Indeed, the QDT $B(R)$ function for the Π states almost coincides with its FDT counterpart, while for the Σ states the QDT result is close to the *ab initio* one at small internuclear distances only, and diverges at $R \geqslant 2.5$ a.u. The latter is attributed to the increase in ionic character in the *ab initio* WF of the lowest $b^3\Sigma_u^+$ state as R increases. Therefore, the single-center $p\sigma$ Coulomb WF used in the QDT model to approximate the $b^3\Sigma_u^+$ state is not valid at $R \geqslant 2.5$. The analogous situation takes place for singlet counterparts of the triplet states [35]. The present $B(R)$ matrix elements between Σ states are in quantitative agreement with the result of model calculations performed in Ref. [22].

The resulting *ab initio* and QDT dipole moment functions for $e\,^3\Sigma_u^+$-$a\,^3\Sigma_g^+$ and $d\,^3\Pi_u$-$a\,^3\Sigma_g^+$ transitions are presented in Figs. 4(a) and 4(b), respectively. At small and medium internuclear distances the QDT functions for both transitions are very close to their *ab initio* counterparts, and slowly diverge as R increases. The latter is not surprising since the

TABLE II. The QDT adiabatic correction $A_{ad}(R)$ for the H_2 $c\,^3\Pi_u$ state calculated by Eq. (11), and the empirical adiabatic IPA potentials for the $d\,^3\Pi_u$ state of H_2 ($Te=110520.36$ cm^{-1}) and D_2 ($Te=111180.40$ cm^{-1}) constructed by the experimental term values from Refs. [7,8]. Internuclear distance R in a.u., energy in cm^{-1}.

R	$A_{ad}[c\,^3\Pi_u(H_2)]$	IPA$[d\,^3\Pi_u(H_2)]$	IPA$[d\,^3\Pi_u(D_2)]$
1.10	84.456	23226.67	23183.41
1.20	81.164	16034.73	16011.71
1.30	78.212	10805.27	10793.57
1.40	75.567	7025.82	7019.73
1.50	73.196	4332.42	4328.88
1.60	71.073	2462.16	2459.79
1.70	69.171	1221.84	1220.14
1.80	67.469	467.18	466.06
1.90	65.947	88.86	88.33
1.95	65.248	13.83	13.62
1.96	65.113	6.79	6.65
2.00	64.588	3.05	3.17
2.05	63.965	48.84	49.28
2.10	63.377	144.56	145.31
2.20	62.300	463.38	464.23
2.30	61.347	917.21	918.60
2.40	60.507	1475.00	1476.84
2.50	59.770	2110.12	2112.84
2.60	59.130	2803.97	2807.02
2.80	58.107	4301.62	4305.23
3.00	57.390	5868.60	5872.77
3.25	56.860	7828.57	7833.48
3.50	56.675	9717.74	9723.44
3.75	56.780	11490.13	11496.21
4.00	57.122	13119.51	13125.51
4.25	57.656	14593.50	14598.52
4.50	58.337	15909.13	15911.61
5.00	59.966	18075.97	18069.67
5.50	61.682	19690.48	19668.39
6.00	63.221	20873.24	20828.26

TABLE III. The experimental and theoretical $Y=|\langle v'|d|v''\rangle/\langle v'|d|v'''\rangle|^2$ ratios for the $d\,^3\Pi_u^-(v') \rightarrow a\,^3\Sigma_g^+(v'';v''')$ transition in H_2 and D_2 calculated by *ab initio* and QDT dipole moments as well as those extracted from the experimental relative intensity distributions in Ref. [12].

v'	v''	v'''	Experiment	QDT	*ab inito*
			H_2		
0	1	0	0.094(0.005)	0.111	0.114
1	0	1	0.056(0.002)	0.049	0.047
1	2	1	0.268(0.015)	0.249	0.257
2	0	2	0.0038(0.0003)	0.0029	0.0027
2	0	2	0.0030(0.0002) [a]	0.0029	0.0027
2	1	2	0.140(0.005)	0.112	0.106
2	1	2	0.120(0.003) [a]	0.112	0.106
2	3	2	0.41(0.02)	0.427	0.439
3	1	3	0.0168(0.0008)	0.011	0.010
3	1	3	0.0095(0.0005) [a]	0.011	0.010
3	2	3	0.219(0.006)	0.189	0.179
3	2	3	0.180(0.004) [a]	0.189	0.179
3	4	3	0.65(0.03)	0.661	0.679
4	3	4	0.34(0.02)	0.287	0.270
4	5	4	0.93(0.06)	0.977	1.003
5	4	5	0.44(0.02)	0.409	0.382
5	6	5	1.51(0.08)	1.413	1.444
6	4	6	0.15(0.01)	0.109	0.098
6	5	6	0.62(0.03)	0.559	0.519
			D_2		
0	1	0	0.145(0.004)	0.140	0.143
1	0	1	0.084(0.005)	0.0852	0.0825
1	2	1	0.310(0.009)	0.328	0.335
2	1	2	0.210(0.006)	0.194	0.187
2	3	2	0.57(0.03)	0.588	0.599
3	2	3	0.38(0.01)	0.336	0.324
3	4	3	0.91(0.05)	0.959	0.977
4	3	4	0.56(0.03)	0.529	0.507
4	5	4	1.62(0.15)	1.515	1.539
5	4	5	0.85(0.04)	0.805	0.767
5	6	5	2.49(0.15)	2.394	2.422

[a]Experimental data from Ref. [11].

expectation value of the remote electron distance $\overline{r} \approx (3\nu^2 - l(l+1))/2$ for the first member of the Rydberg series $2s\sigma$ corresponding to the $a\,^3\Sigma_g^+$ state becomes comparable with the internuclear distance at $R \geqslant 5$ a.u. [26]. At the same time, the QDT approach allows one to estimate the dipole moment at very small internuclear distances and in the united-atom (UA) limit. Moreover, the difference between experimental and QDT data obtained in the UA limit can be considered as an independent accuracy test of the derived molecular moments at small R values. Indeed, the experimental dipole moment of the $3\,^3P-2\,^3S$ He I atomic transition, which is the UA limit for both e-a and d-a molecular transitions, is equal to 0.524 a.u. [43], while its QDT counterpart estimated by the ν values of the corresponding He I atomic states [43] is 0.557 a.u. Hence the absolute accuracy of the QDT moments for the above-mentioned transitions is better than 0.05 a.u. at small internuclear distances. Both theoretical functions are in reasonable agreement with their empirical analogs near equilibrium points of the interacting states. The divergency increases rapidly as R increases, especially regarding the e-a transition. This should be attributed to an extrapolation error in the empirical functions beyond the experimental data range used for their construction.

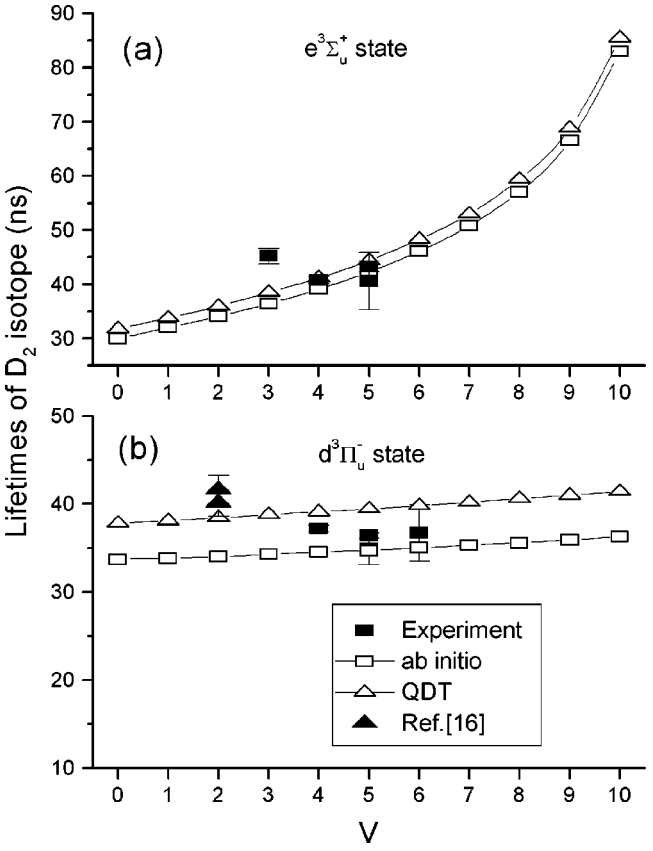

FIG. 5. Experimental and calculated radiative lifetimes of the $e\,^3\Sigma_u^+$ (a) and $d\,^3\Pi_u^-$ (b) states of D_2. The predissociation effect is negligible in both states.

The adiabatic corrections obtained by Eq. (11) for the H_2 $c\,^3\Pi_u$ state together with the derived IPA potential curves for H_2 and D_2 $d\,^3\Pi_u$ states are presented in Table II. To construct the IPA potentials, only Π^- term values were used because they do not undergo the L-uncoupling perturbation effect, unlike the Π^+ ones. The derived adiabatic potentials of the $c\,^3\Pi_u$ state reproduce the experimental term value positions of the $c\,^3\Pi_u^-$ state for both isotopes [7,8], with a mean-squared deviation (s.d.) of 0.5 cm^{-1}. This gives us absolute insurance in the high accuracy of the repulsive wall of the derived adiabatic potentials for the $c\,^3\Pi_u$ state. The derived IPA potentials fit the relevant experimental rovibronic term values for H_2 $(0 \leqslant v' \leqslant 9, 1 \leqslant N' \leqslant 8)$ and D_2 $(0 \leqslant v' \leqslant 10, 1 \leqslant N' \leqslant 18)$ $d\,^3\Pi_u$ levels [7,8] with 0.11 and 0.15 cm^{-1} s.d., respectively.

The required vibrational WF's of the $d\,^3\Pi_u^-$ and Σ states were obtained from Eq. (10) with IPA potentials and full *ab initio* adiabatic potentials taken from Refs. [18] and [19], respectively. To test the IPA potential curves for the $d\,^3\Pi_u^-$ state as well as the derived QDT and *ab initio* $d(R)$ functions for the d-a transition, the vibronic $\langle v'|d|v''\rangle$ matrix elements for both isotopes were calculated and are compared

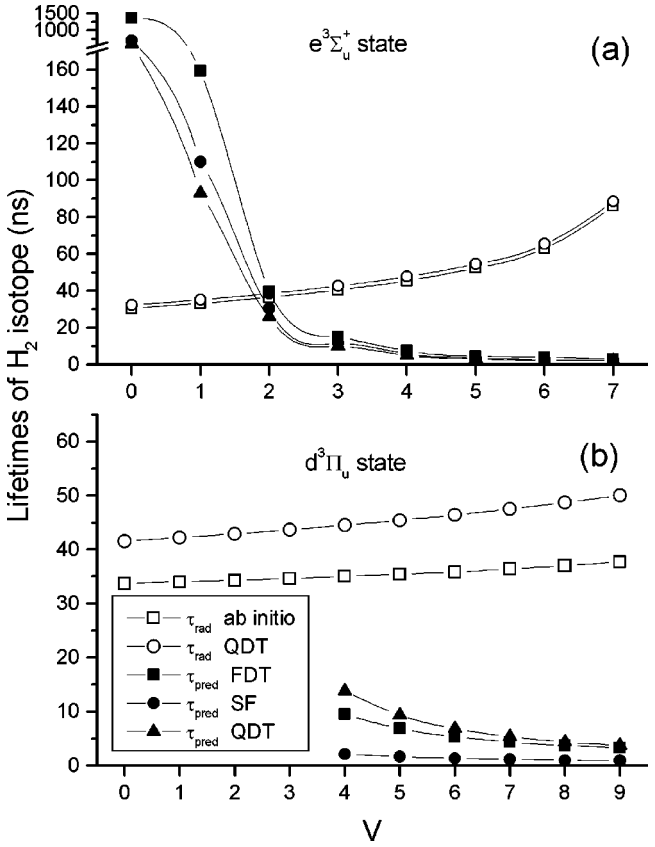

FIG. 6. Predissociative and radiative lifetimes of the $e\,^3\Sigma_u^+(N'=0)$ (a) and $d\,^3\Pi_u^-(N'=1)$ (b) states of H_2 calculated with *ab initio* and QDT radial coupling and dipole moment functions.

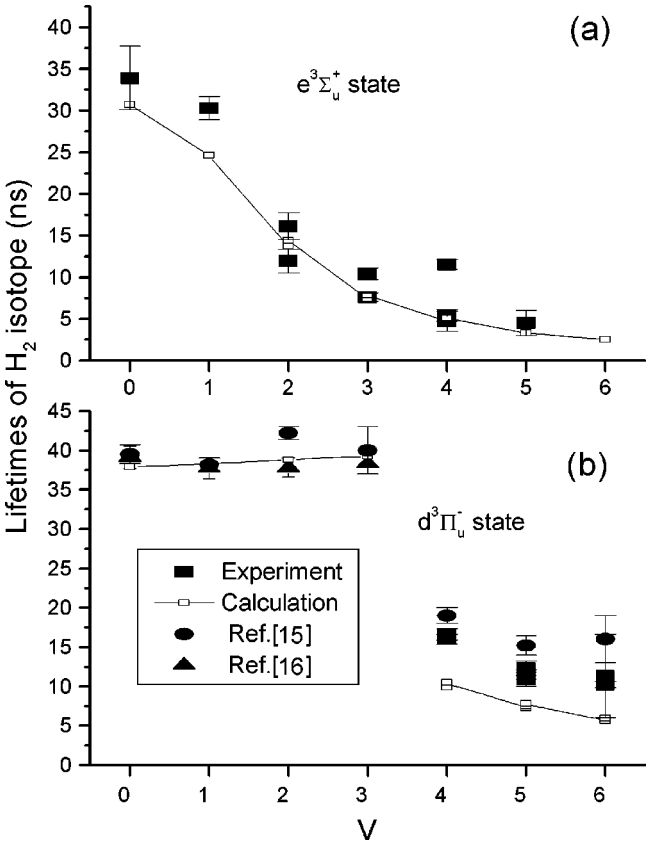

FIG. 7. Experimental and theoretical lifetimes of the $e\,^3\Sigma_u^+$ (a) and $d^3\Pi_u^-$ (b) states of H_2. The theoretical lifetimes were derived based on the dipole moments calculated by the *ab initio* method and the coupling matrix elements calculated by the *ab initio* FDT method.

in Table III with the experimental data extracted from relative intensity distribution in emission of the $d\,^3\Pi_u^- \rightarrow a\,^3\Sigma_g^+$ transition [11,12]. A good agreement between the experimental and theoretical data obtained by both QDT and *ab initio* $d(R)$ functions gives us an additional insurance concerning the derived IPA potentials for both isotopes since the overlap integrals $\langle v'|v''\rangle$ are very sensitive to the accuracy of the potentials used [44]. The pure radiative lifetime values calculated using Eq. (1) are presented in Figs. 5 and 6. The mass dependence of the radiative lifetime values was found to be negligible for both the $e\,^3\Sigma_u^+$ and $d\,^3\Pi_u$ states. This proves the validity of the adiabatic approximation in the radiative lifetime case. The N' dependence of the $\tau_{\rm rad}$ values was found to be almost negligible for N' values up to 5 as well, while the corresponding vibronic matrix elements $\langle v'|d|v''\rangle$ for both transitions showed pronounced mass and N' dependences. The obtained pure radiative lifetimes for all levels of $e\,^3\Sigma_u^+$ and $d\,^3\Pi_u$ states of D_2 are in good agreement with the relevant experimental data as seen in Figs. 5(a) and 5(b). This means that the deuterium states undergo radiative decay only. The experimental lifetimes for H_2 $d\,^3\Pi_u^-(v'\leqslant 3)$ levels lying below the dissociation limit of the perturbing $c\,^3\Pi_u$ state [15,16] agree well with their theoretical counterparts derived by both QDT and *ab initio* *d-a* dipole moment functions [see Fig. 7(b)]. The calculated $\tau_{\rm rad}$ values for the $e\,^3\Sigma_u^+$ state also confirm the indirect lifetime estimates derived by the relative intensity measurements in Refs. [3,10].

The predissociation rates of the rovibronic $e\,^3\Sigma_u^+$ and $d\,^3\Pi_u^-$ levels of H_2 and D_2 have been estimated by a combination of Eqs. (2) and (12) using the theoretical radial coupling functions $B(R)$ mentioned above. The relevant bound and continuum vibrational WF's were obtained from Eq. (10) with *ab initio* adiabatic potentials for Σ states [19], with IPA potentials from Table II for the $d\,^3\Pi_u$ state and with the BO potential [20] plus the QDT adiabatic correction from Table II for the $c\,^3\Pi_u$ state. The results for $e\,^3\Sigma_u^+(v'\geqslant 0; N'=0)$ and $d\,^3\Pi_u^-(v'\geqslant 4; N'=1)$ levels of H_2 derived with different $B(R)$ functions are presented in Figs. 6(a) and 6(b). For both states studied the predissociation rates were found to be almost independent of the N' values, and rapidly increased as v' values increased. However, the absolute magnitude of the predissociation rates is very small comparable to the radiative decay rates even at the highest vibrational levels. Moreover, the $\tau_{\rm pred}^{-1}$ values for D_2 are approximately 10^3 times smaller than those for H_2. Thus, as expected, the predissociation decay channel is negligible in comparison with the radiative one for D_2. It is interesting that the calculated predissociation rates cannot be simply explained by explicit mass dependence of relation (2). The main contribution in the dependence of $\tau_{\rm pred}$ on the reduced mass comes from the exceptional sensitivity of the exponentially small differential Franck-Condon factor $|\langle \chi_{v'N'}|d\chi_{E''N'}/dR\rangle|^2$ to the nodal structure of $\chi_{v'N'}(R)$ and $\chi_{E''N'}(R)$ vibrational WF's in the R region near the

maximum $B_{ij}(R)$ function. A sum of both predissociative and radiative decay rates for H_2 $e\,^3\Sigma_u^+(v' \geqslant 0)$ and $d\,^3\Pi_u^-(v' \geqslant 4)$ levels, presented in Figs. 7(a) and 7(b), are in reasonable agreement with the experimental lifetimes.

V. CONCLUSIONS

An overall quantitative agreement between the experimental lifetimes measured by a delayed coincidence method for $e\,^3\Sigma_u^+$ and $d\,^3\Pi_u^-$ states of both isotopes, and the theoretical results obtained based on the assumed competition between radiative and predissociative decay have been achieved in the present study. The predissociative rates for both $e\,^3\Sigma_u^+(v' \geqslant 0)$ and $d\,^3\Pi_u^-(v' \geqslant 4)$ states of H_2 rapidly increase as the v' value increases, and become comparable with the radiative decay rates, while for D_2, the predissociation effect is negligible for both states and the experimental lifetimes correspond to the radiative decay channel only.

However, there still exists a slight difference of absolute values between the experimental and theoretical data for the H_2 $d^3\Pi_u^-(v' \geqslant 4)$ levels, and in addition localized variations of the experimental lifetimes with the N' values have been observed as in a different tendency from the theoretical results for H_2 $e\,^3\Sigma_u^+(v'=2,3,4)$ levels [see Table I and Figs. 7(a) and 7(b)]. More accurate *ab initio* calculations of the radial coupling and dipole transition matrix elements are necessary to remove the observed discrepancy for the $d\,^3\Pi_u^-$ levels. Furthermore, the lifetime variation with the N' values seems attributable to both homogeneous and heterogeneous perturbation effects among $e\,^3\Sigma_u^+$, $d\,^3\Pi_u$, $f\,^3\Sigma_u^+$, and $k\,^3\Pi_u$ 3,4*p*-complex triplet states, in addition to predissociations through $b\,^3\Sigma_u^+$ and $c\,^3\Pi_u^-$ states. For instance, for N' dependence of lifetimes of the $e\,^3\Sigma_u^+(v'=4)$ levels, a qualitative explanation is possible by considering the strong local *L*-uncoupling perturbation effect from the $d\,^3\Pi_u^+(v'=1)$ levels [16]. Therefore, in order to obtain more of an insight into the nonadiabatic behavior of an ungerade triplet *p* complex, simultaneous treatment of all participated states mentioned above is certainly required, instead of the present two-level interaction treatment. In particular, extensive *ab initio* calculations with a huge GTO basis set together with a direct numerical solution of channel-coupling equations among these states is now in progress. Further accumulation of experimental lifetime data and emission intensities is also necessary. This involves systematic lifetime measurements for the triplet 4*p*-complex levels and improvement in experimental accuracy.

ACKNOWLEDGMENTS

Financial support of this work by the Russian Foundation of Basic Research under Grant Nos. 97-03-32215a and 97-03-33714a is gratefully acknowledged by three of the authors (S.A., E.P., and A.S.). We thank Laboratoire de Physique Quantique (Toulouse) for providing their MRCI program used to calculate FCI WF's. We are especially grateful to Professor Andrej V. Zaitsevskii (Moscow) for his considerable help in performing the *ab initio* calculations and for useful discussions. We thank Professor M.S. Child (Oxford) and Professor L. Wolniewicz (Torun) for their critical reading of the manuscript.

[1] J.L. Terry, J. Vac. Sci. Technol. A **1**, 831 (1983).
[2] J.M. Ajello, S.K. Srivastava, and J.L. Yunag, Phys. Rev. A **25**, 2485 (1982).
[3] S.A. Astashkevich, M. Käning, E. Käning, N.V. Kokina, B.P. Lavrov, A. Ohl, and J. Pöpcke, J. Quant. Spectrosc. Radiat. Transf. **56**, 725 (1996).
[4] W. Kolos and L. Wolniewicz, Rev. Mod. Phys. **35**, 473 (1963).
[5] H. Lefebvre-Brion and R.W. Field, *Perturbations in the Spectra of Diatomic Molecules* (Academic Press, New York, 1986).
[6] G.H. Dieke, J. Mol. Spectrosc. **2**, 494 (1958).
[7] N.Y. Crosswhite, *The Hydrogen Molecule Wavelength Tables of G. H. Dieke* (Wiley, New York, 1972).
[8] R.S. Freund, J.A. Schiavone, and N.Y. Crosswhite, J. Phys. Chem. Ref. Data **14**, 235 (1985).
[9] I. Kovács, B.P. Lavrov, M.V. Tyutchev, and V.I. Ustimov, Acta Phys. Hung. **54**, 161 (1983).
[10] B.P. Lavrov, M.V. Tyutchev, and V.I. Ustimov, Opt. Spektrosk. **64**, 1251 (1988) [Opt. Spectrosc. **64**, 745 (1988)].
[11] T.V. Kirbyateva, B.P. Lavrov, V.N. Ostrovskii, M.V. Tyutchev, and V.I. Ustimov, Opt. Spectrosk. **52**, 39 (1982) [Opt. Spectrosc. **52**, 21 (1982)].
[12] B.P. Lavrov and L.L. Pozdeev, Opt. Spektrosk. 66, 818 (1989) [Opt. Spectrosc. **66**, 479 (1989)].
[13] S.A. Astashkevich, B.P. Lavrov, L.L. Pozdeev, and V.I. Ustimov, Opt. Spektrosk. **70**, 285 (1991) [Opt. Spectrosc. **70**, 164 (1991)].
[14] R.L. Day, R.J. Anderson, and F.A. Sharpson, J. Chem. Phys. **69**, 5518 (1978); I.P. Bogdanova, G.V. Efremova, B.P. Lavrov, V.N. Ostrovskii, V.I. Ustimov, and V.I. Yakovleva, Opt. Spektrosk. **50**, 121 (1981) [Opt. Spectrosc. **50**, 63 (1981)]; T. Kiyoshima, J. Phys. Soc. Jpn. **56**, 1989 (1987); A. Sanchez and J. Campos, J. Phys. (Paris) **49**, 445 (1988).
[15] M.L. Burshtein, B.P. Lavrov, A.S. Melnikov, V.P. Prosikhin, S.V. Yurgenson, and V.N. Yakovlev, Opt. Spektrosk, **68**, 285 (1990) [Opt. Spectrosc. **68**, 166 (1990).
[16] T. Kiyoshima and H. Sato, Phys. Rev. A **48**, 4771 (1993).
[17] B. Meierjohann and M. Volger, Phys. Rev. A **17**, 47 (1978).
[18] W. Kolos and J. Rychlewski, J. Mol. Spectrosc. **169**, 341 (1995).
[19] W. Kolos and J. Rychlewski, J. Mol. Spectrosc. **143**, 237 (1990).
[20] W. Kolos and J. Rychlewski, J. Mol. Spectrosc. **66**, 428 (1977).
[21] S.R. Langhoff, W.M. Huo, H. Partridge, and C.W. Bauschlicherz, J. Chem. Phys. **77**, 2498 (1982).
[22] F. Borondo, F. Martin, and M. Yanez, J. Chem. Phys. **86**, 4982 (1987).
[23] S.W. Provencher, J. Chem. Phys. **64**, 2772 (1976).
[24] N.H. Gale, Nucl. Phys. **38**, 252 (1962).
[25] E.E. Eyler and F.M. Pipkin, Phys. Rev. Lett. **47**, 1270 (1981); J.M. Schins, L.D.A. Siebbels, J. Los, and W.J. van der Zande, Phys. Rev. A **44**, 4162 (1991); M.D. Ray and G.P. Lafyatis, Phys. Rev. Lett. **76**, 2662 (1996).
[26] A.V. Stolyarov and M.S. Child, J. Phys. B **32**, 527 (1999).

[27] L. Engström, Nucl. Instrum. Methods Phys. Res. **202**, 369 (1982).
[28] M.S. Child, in *Molecular Spectroscopy*, edited by R.F. Barrow, D.A. Long, and D.J. Mollen (Chemical Society, London, 1974), Vol. 2, p. 466.
[29] Ch. Jungen and O. Atabek, J. Chem. Phys. **66**, 5584 (1977).
[30] P.O. Wildmark, B.J. Persson, and B.O. Ross, Theor. Chim. Acta **79**, 419 (1991).
[31] C. Galloy and J.C. Lorquet, J. Chem. Phys. **67**, 4672 (1977); G. Hirsch, P.J. Bruna, R.J. Buenker, and S.D. Peyerimhoff, *ibid.* **45**, 335 (1980).
[32] V. Sidis, J. Chem. Phys. **55**, 5838 (1971).
[33] M.J. Seaton, Rep. Prog. Phys. **46**, 167 (1983).
[34] R.S. Mulliken, J. Am. Chem. Soc. **86**, 3183 (1964).
[35] A.V. Stolyarov, V.I. Pupyshev, and M.S. Child, J. Phys. B **30**, 3077 (1997).
[36] D.M. Bishop and R.W. Wetmore, Mol. Phys. **26**, 145 (1973).
[37] D.R. Bates and A. Damgaard, Philos. Trans. R. Soc. London, Ser. A **242**, 101 (1949).
[38] R.S. Mulliken, J. Chem. Phys. **33**, 247 (1960).
[39] W.M. Kosman and J. Hinze, J. Mol. Spectrosc. **56**, 93 (1975); C.R. Vidal and H. Scheingraber, *ibid.* **65**, 46 (1977).
[40] B.R. Johnson, J. Chem. Phys. **67**, 4086 (1977).
[41] L.F. Richardson, Philos. Trans. R. Soc. London, Ser. A **226**, 299 (1927).
[42] A.V. Abarenov and A.V. Stolyarov, J. Phys. B **23**, 2419 (1990).
[43] *Atomic Transition Probabilities*, edited by W.L. Wiese, M.W. Smith, and B.M. Glennon, Natl. Bur. Stand. Tech. News Bull. U.S. NBS No. 4 (U.S. GPO, Washington, DC, 1966).
[44] E.A. Pazuyk, A.V. Stolyarov, I.V. Ushakov, and R.S. Ferber, J. Quant. Spectrosc. Radiat. Transf. **53**, 565 (1995).